Available online at www.sciencedirect.com

SCIENCE DIRECT®

International Journal of Heat and Mass Transfer 47 (2004) 5619–5627

International Journal of HEAT and MASS TRANSFER

www.elsevier.com/locate/ijhmt

Analysis of mixed convection in a vertical porous layer using non-equilibrium model

Nawaf H. Saeid *

School of Mechanical Engineering, University of Science Malaysia, 14300 Nibong Tebal, Pulau Pinang, Malaysia

Received 26 February 2004; received in revised form 20 July 2004

Abstract

The problem of two-dimensional steady mixed convection in a vertical porous layer is investigated numerically in the present paper using the thermally non-equilibrium model. The vertical porous layer is assumed to have a finite isothermally heated segment on one vertical wall which is otherwise adiabatic and the other vertical wall is cooled to a constant temperature. Non-dimensionalization of the governing equations results in four parameters for both aiding and opposing flows: (1) Ra, Rayleigh number (2) Pe, Péclet number (3) K_r, thermal conductivity ratio parameter, and (4) H, heat transfer coefficient parameter. The numerical results are presented for $0.01 \leqslant H \leqslant 100$, $0.01 \leqslant K_r \leqslant 100$, $0.01 \leqslant Pe \leqslant 100$ and $Ra = 10$, 50 and 100. The results show that, the thermal equilibrium model cannot predict the average Nusselt number correctly for small values of $H \times K_r$. In both the aiding and opposing flows, the total average Nusselt number is decreasing with increasing the heat transfer coefficient parameter at low values of Pe, while for high values of Pe, higher H will enhance the total heat transfer rate. Increasing the thermal conductivity ratio leads to increase in the total average Nusselt number. It is found also that the total average Nusselt number depends strongly on the thermal conductivity ratio parameter and depends slightly on the heat transfer coefficient parameter.

1. Introduction

Convective heat transfer in vertical or horizontal porous layers has attracted attention of various researchers during the last five decades in view of several very distinct advantages of such a transport process in modern technologies. The applications include, for example, electronic systems cooling, petroleum reservoirs, geothermal reservoir, grain storage, fiber and granular insulation, etc. Several excellent review articles and monographs summarizing the state-of-the-art available in the literature testify to the maturity of convection in porous media in general (see for example, [1–5]). Various essential characteristics of steady mixed convection in a two-dimensional horizontal or vertical porous layers has been studied in several papers by Lai et al. [6–8], Lai and Kulacki [9], Lai [10] and Prasad et al. [11]. In these papers, the thermal equilibrium model is assumed, i.e., the temperature of the solid and the fluid are assumed to be the same within the representative control volume. Thermal equilibrium in convection in porous media is not valid for many cases as reported by various authors for different applications [12–14]. It is expected that, when there is a significant difference between advection and conduction mechanisms in transferring heat, the deviation between solid and fluid phase temperatures increases.

* Tel.: +60 4 593 7788; fax: +60 4 594 1025.
E-mail address: n_h_saeid@yahoo.com

0017-9310/$ - see front matter © 2004 Elsevier Ltd. All rights reserved.
doi:10.1016/j.ijheatmasstransfer.2004.07.033

Nomenclature

c_p	specific heat, $\mathrm{J\,kg^{-1}\,K^{-1}}$
g	gravitational acceleration, $\mathrm{m\,s^{-2}}$
h	volumetric heat transfer coefficient, $\mathrm{W\,m^{-3}\,K^{-1}}$
H	heat transfer coefficient parameter, defined in Eq. (10)
L	heat source length, m
k	thermal conductivity, $\mathrm{W\,m^{-1}\,K^{-1}}$
K	permeability, $\mathrm{m^2}$
K_r	thermal conductivity ratio parameter, defined in Eq. (10)
$\overline{Nu}$	average Nusselt number, defined in Eq. (12) or (14)
Pe	Péclet number, defined in Eq. (10)
q''	heat flux, $\mathrm{W\,m^{-2}}$
Ra	Rayleigh number, defined in Eq. (10)
T	temperature, K
u, v	velocity components along x- and y-axis, respectively, $\mathrm{m\,s^{-1}}$
V_0	inlet velocity, $\mathrm{m\,s^{-1}}$
U, V	non-dimensional velocity components, defined in Eq. (6)
x, y	Cartesian coordinates, m
X, Y	non-dimensional Cartesian coordinates, defined in Eq. (6)

Greek symbols

α	thermal diffusivity, $\mathrm{m^2\,s^{-1}}$
β	coefficient of volume expansion, $\mathrm{K^{-1}}$
ν	kinematic viscosity, $\mathrm{m^2\,s^{-1}}$
ρ	density, $\mathrm{kg\,m^{-3}}$
θ	non-dimensional temperature, defined in Eq. (6)
φ	porosity, (void volume/total volume of the porous medium)
Ψ	non-dimensional stream function, defined in Eq. (6)

Subscripts

c	cold wall
h	hot wall
f	fluid
s	solid
t	total (fluid + solid)

Schumann [15] suggested a simple two-equation model to account for non-equilibrium condition for incompressible forced flow in a porous medium. Vafai and Sozen [13], extended the Schumann model to account for compressible flow taking into account of Forchheimer term and conduction effects in the gas and solid phases. Amiri and Vafai [16] presented a detailed analysis for forced flow through channel filled with saturated medium. Their results indicate that the Darcy and particle Reynolds parameters are most influential parameters in determining the validity of the local thermal equilibrium. Recently the non-equilibrium model has been used in the analysis of different convection heat transfer problems in porous media by various authors [17–25]. In the non-equilibrium modeling, it is required to know the volumetric heat transfer coefficient between solid and fluid phases. In the literature there are some attempts to measure volumetric heat transfer coefficient under forced convection conditions [26–28]. In fact, the results depend on the accuracy of the model assumptions and accuracy of the input parameters, such as thermo-physical properties of the solid matrix, effective thermal conductivity, boundary conditions and effect of radiation, etc. No experimental or theoretical analysis could be identified in the literature about volumetric heat transfer coefficient under free or mixed convection conditions. From the basics of heat transfer, it is expected that the volumetric heat transfer coefficient for free convection may be quite low compared with forced convection, unless the Rayleigh parameter is very high. In the present work, the volumetric heat transfer coefficient parameter is assumed to be in a range of 0.01–100 for mixed convection mode. The Darcy model and the non-equilibrium model are used also to study the mixed convection in a vertical porous layer induced by a finite isothermal heat source on one vertical wall in the presence of external flow with the opposite wall moving at constant velocity. Two different cases are considered; one is the aiding flow, when the external flow aids the buoyancy forces on the hot wall, and the other is the opposing flow, which represents the situation when the buoyant flow on the hot wall is opposed by the external forced flow. A schematic diagram of the aiding and opposing flows model along with the coordinate system is shown in Fig. 1.

2. Governing equations

The conservation equations for mass, momentum and energy in two-dimensional, laminar mixed convection flow in porous layer, using the non-equilibrium model are:

$$\frac{\partial u}{\partial x}+\frac{\partial v}{\partial y}=0 \tag{1}$$

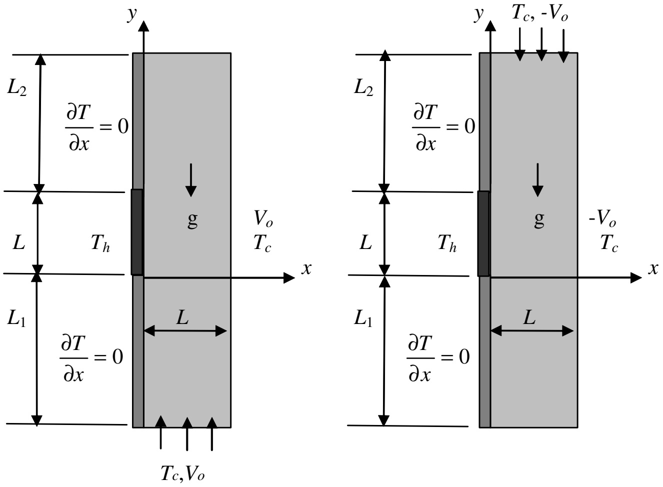

(a) Aiding flow **(b)** Opposing flow

Fig. 1. Schematic diagram of the physical model and coordinate system.

$$\frac{\partial u}{\partial y}-\frac{\partial v}{\partial x}=\frac{-g\beta K}{\nu}\frac{\partial T_{\mathrm{f}}}{\partial y} \tag{2}$$

$$(\rho c_p)_{\mathrm{f}}\left(u\frac{\partial T_{\mathrm{f}}}{\partial x}+v\frac{\partial T_{\mathrm{f}}}{\partial y}\right)=\varphi k_{\mathrm{f}}\left(\frac{\partial^2 T_{\mathrm{f}}}{\partial x^2}+\frac{\partial^2 T_{\mathrm{f}}}{\partial y^2}\right)+h(T_{\mathrm{s}}-T_{\mathrm{f}}) \tag{3}$$

$$(1-\varphi)k_{\mathrm{s}}\left(\frac{\partial^2 T_{\mathrm{s}}}{\partial x^2}+\frac{\partial^2 T_{\mathrm{s}}}{\partial y^2}\right)+h(T_{\mathrm{f}}-T_{\mathrm{s}})=0 \tag{4}$$

where u, v are the velocity components along x- and y-axis, T_{f} is the fluid phase temperature, T_{s} is the solid phase temperature and the physical meaning of the other quantities are mentioned in the nomenclature. Eqs. (1)–(4) are subject to the following boundary conditions:

$$u(0,y)=0,\quad T_{\mathrm{f}}(0,y)=T_{\mathrm{s}}(0,y)=T_{\mathrm{h}}\quad \text{for } 0\leqslant y\leqslant L;$$

and

$$\frac{\partial T_{\mathrm{f}}(0,y)}{\partial x}=\frac{\partial T_{\mathrm{s}}(0,y)}{\partial x}=0\quad \text{for } y<0,\ y>L \tag{5a}$$

$$\begin{aligned}&u(L,y)=0,\quad T_{\mathrm{f}}(L,y)=T_{\mathrm{s}}(L,y)=T_{\mathrm{c}}\\&v(L,y)=V_0\quad \text{for aiding flow,}\\&\text{and}\quad v(L,y)=-V_0\quad \text{for opposing flow}\end{aligned} \tag{5b}$$

$$\begin{aligned}&u(x,-L_1)=0,\quad v(x,-L_1)=V_0,\\&T_{\mathrm{f}}(x,-L_1)=T_{\mathrm{s}}(x,-L_1)=T_{\mathrm{c}}\quad \text{for aiding flow}\\&u(x,-L_1)=0,\quad \frac{\partial v(x,-L_1)}{\partial y}=\frac{\partial T_{\mathrm{f}}(x,-L_1)}{\partial y}\\&\quad=\frac{\partial T_{\mathrm{s}}(x,-L_1)}{\partial y}=0\quad \text{for opposing flow}\end{aligned} \tag{5c}$$

$$\begin{aligned}&u(x,L_2)=0,\quad \frac{\partial v(x,L_2)}{\partial y}=\frac{\partial T_{\mathrm{f}}(x,L_2)}{\partial y}\\&\quad=\frac{\partial T_{\mathrm{s}}(x,L_2)}{\partial y}=0\quad \text{for aiding flow}\\&u(x,L_2)=0,\quad v(x,L_2)=-V_0,\\&T_{\mathrm{f}}(x,L_2)=T_{\mathrm{s}}(x,L_2)=T_{\mathrm{c}}\quad \text{for opposing flow}\end{aligned} \tag{5d}$$

It is assumed that the fluid and solid phases share the same temperature as that of the vertical isothermal walls, i.e., equilibrium condition is imposed on the non-permeable walls. The values of L_1 and L_2 are taken large enough so that the boundary conditions (5c) and (5d) will be realistic at the inlet and exit of the porous layer. The governing equations (1)–(4) can be written in non-dimensional form by using the following non-dimensional variables:

$$X=\frac{x}{L};\quad Y=\frac{y}{L};\quad U=\frac{u}{V_0}=\frac{\partial\Psi}{\partial Y};\quad V=\frac{v}{V_0}=\frac{-\partial\Psi}{\partial X};\quad \theta=\frac{T-T_{\mathrm{c}}}{\Delta T} \tag{6}$$

where $\Delta T=(T_{\mathrm{h}}-T_{\mathrm{c}})$. The resulting dimensionless forms of the governing equations are as follows:

$$\frac{\partial^2\Psi}{\partial Y^2}+\frac{\partial^2\Psi}{\partial X^2}=\frac{-Ra}{Pe}\frac{\partial\theta_{\mathrm{f}}}{\partial X} \tag{7}$$

$$Pe\left(\frac{\partial\Psi}{\partial Y}\frac{\partial\theta_{\mathrm{f}}}{\partial X}-\frac{\partial\Psi}{\partial X}\frac{\partial\theta_{\mathrm{f}}}{\partial Y}\right)=\left(\frac{\partial^2\theta_{\mathrm{f}}}{\partial X^2}+\frac{\partial^2\theta_{\mathrm{f}}}{\partial Y^2}\right)+H(\theta_{\mathrm{s}}-\theta_{\mathrm{f}}) \tag{8}$$

$$\frac{\partial^2\theta_{\mathrm{s}}}{\partial X^2}+\frac{\partial^2\theta_{\mathrm{s}}}{\partial Y^2}+HK_r(\theta_{\mathrm{f}}-\theta_{\mathrm{s}})=0 \tag{9}$$

where, the parameters arises in the non-dimensionlization are defined as:

$$Ra = \frac{g\beta K \Delta T L}{\varphi \nu \alpha_f}; \quad Pe = \frac{V_0 L}{\varphi \alpha_f};$$
$$K_r = \frac{\varphi k_f}{(1-\varphi)k_s}; \quad H = \frac{hL^2}{\varphi k_f} \tag{10}$$

The boundary conditions (5) become:

$$\Psi(0, Y) = 0,$$

$$\theta_f(0, Y) = \theta_s(0, Y) = 1 \quad \text{at } 0 \leqslant Y \leqslant 1$$

and

$$\frac{\partial \theta_f(0, Y)}{\partial X} = \frac{\partial \theta_s(0, Y)}{\partial X} = 0 \quad \text{at } Y < 0, \; Y > 1 \tag{11a}$$

$$\theta_f(1, Y) = \theta_s(1, Y) = 0$$

$$\Psi(1, Y) = -1 \text{ for aiding flow}$$

and

$$\Psi(1, Y) = 1 \text{ for opposing flow} \tag{11b}$$

$$\begin{aligned} &\theta_f(X, -Y_1) = \theta_s(X, -Y_1) = 0, \\ &\Psi(X, -Y_1) = -X \quad \text{for aiding flow} \\ &\frac{\partial \Psi(X, -Y_1)}{\partial Y} = \frac{\partial \theta_f(X, -Y_1)}{\partial Y} \\ &\quad = \frac{\partial \theta_f(X, -Y_1)}{\partial Y} = 0 \quad \text{for opposing flow} \end{aligned} \tag{11c}$$

$$\begin{aligned} &\frac{\partial \Psi(X, Y_2)}{\partial Y} = \frac{\partial \theta_f(X, Y_2)}{\partial Y} \\ &\quad = \frac{\partial \theta_s(X, Y_2)}{\partial Y} = 0 \quad \text{for aiding flow} \\ &\theta_f(X, Y_2) = \theta_s(X, Y_2) = 0, \\ &\Psi(X, Y_2) = X \quad \text{for opposing flow} \end{aligned} \tag{11d}$$

The physical quantities of interest in the present problem are the average Nusselt number for the fluid and solid phases at the heated wall segment, defined by:

$$\overline{Nu_f} = \int_0^1 -\left(\frac{\partial \theta_f}{\partial X}\right)_{X=0} \mathrm{d}Y \tag{12a}$$

$$\overline{Nu_s} = \int_0^1 -\left(\frac{\partial \theta_s}{\partial X}\right)_{X=0} \mathrm{d}Y \tag{12b}$$

It is of practical importance to determine the average total heat transfer (by fluid and solid) per unit area from the heated segment, which can be calculated as:

$$\begin{aligned} \overline{q_t''} &= \frac{1}{L}\int_0^L q_t''(y)\,\mathrm{d}y \\ &= \frac{-1}{L}\int_0^L \left\{\varphi k_f \left(\frac{\partial T_f}{\partial x}\right)_{x=0} + (1-\varphi)k_s\left(\frac{\partial T_s}{\partial x}\right)_{x=0}\right\}\mathrm{d}y \end{aligned} \tag{13}$$

From which it can be shown that, the total average Nusselt number is:

$$\begin{aligned} \overline{Nu_t} &= \frac{\overline{q_t''}L}{\Delta T\{\varphi k_f + (1-\varphi)k_s\}} \\ &= \frac{-1}{(K_r+1)}\int_0^1 \left\{K_r\left(\frac{\partial \theta_f}{\partial X}\right)_{X=0} + \left(\frac{\partial \theta_s}{\partial X}\right)_{X=0}\right\}\mathrm{d}Y \end{aligned} \tag{14}$$

3. Numerical scheme

Eqs. (7)–(9) subjected to the boundary conditions (11) are integrated numerically using the finite volume method, which is described in the book by Patankar [29]. The central differencing scheme is used for the diffusion terms of the energy equations (8) and (9) as well as in the momentum equation (7). The quadratic upwind differencing QUICK scheme given by Hayase et al. [30] is used for the convection terms formulation of the energy equation of the fluid phase (8). This scheme has a third-order accurate approximation for the uniform grid spacing. The linear extrapolation, known as mirror node approach, has been used for the boundary conditions implementation. The resulting algebraic equations were solved by line-by-line using the Tri-Diagonal Matrix Algorithm iteration. The iteration process is terminated under the following condition:

$$\sum_{i,j} |\phi_{i,j}^n - \phi_{i,j}^{n-1}| \Big/ \sum_{i,j} |\phi_{i,j}^n| \leqslant 10^{-5} \tag{15}$$

where ϕ is the general dependent variable which can stands for θ_f, θ_s or Ψ and n denotes the iteration step. In the present study, the mesh is selected to be same as that used by Lai et al [7]; which is 21×201, 21×301, 21×401 equal spacing grids for $Ra = 10$, 50 and 100, respectively. The length on the upstream and down stream sides of the heat source (Y_1 and Y_2), have been varied with Péclet number and flow direction. To check the accuracy of the present numerical method, the results of the present numerical scheme obtained for the case of the equilibrium conditions is compared with the results of the thermally equilibrium model used by Lai et al. [7]. The average Nusselt number for the fluid phase $\overline{Nu_f}$ has been calculated and listed in Table 1 along with the results of Lai et al. [7]. The temperature gradient at the wall has been calculated using three point expression which has third order accuracy also. The maximum discrepancy between the present results and Lai et al. [7] results is less than 2%. These results provide confidence to the accuracy of the developed code for both aiding and opposing flows and it is used to generate results for the non-equilibrium model.

Table 1
Comparison of the average Nusselt number of the equilibrium model with the results of Lai et al. [7]

Flow	Ra	Pe = 0.01		Pe = 1		Pe = 10		Pe = 100	
		Ref. [7]	Present	Ref. [7]	Present	Ref. [7]	Present	Ref. [7]	Present
Aiding flow	10	2.08	2.04	2.27	2.24	4.22	4.20	11.63	11.73
	50	4.07	4.01	4.33	4.28	6.23	6.18	12.63	12.82
	100	6.34	6.29	6.57	6.52	8.26	8.20	13.84	13.98
Opposing flow	10	2.08	2.04	1.96	1.93	3.22	3.17	11.08	11.12
	50	4.06	4.03	3.80	3.76	2.41	2.37	9.86	9.88
	100	6.34	6.39	6.10	6.14	4.17	4.13	8.28	8.21

4. Results and discussion

The results were obtained for Rayleigh number $Ra = 10$, 50 and 100 where Darcy model is applicable and Péclet number for mixed convection range of $0.01 \leqslant Pe \leqslant 100$. The results are found to show the effect of the two parameters arising from the thermally non-equilibrium between the solid and fluid phases, which are the heat transfer coefficient parameter in the range $0.01 \leqslant H \leqslant 100$ and thermal conductivity ratio parameter in the range $0.01 \leqslant K_r \leqslant 100$ for both aiding and opposing flows.

4.1. Effect of heat transfer coefficient parameter H

Fig. 2 shows the effect of the heat transfer coefficient parameter defined in Eq. (10) on the average Nusselt number. In this figure, the Rayleigh number is chosen $Ra = 50$ for both aiding and opposing flows and thermal conductivity ratio parameter $K_r = 1$ is selected, where the total average Nusselt number is affected equally by the both solid and fluid temperature fields according to Eq. (14). For small values of the heat transfer coefficient parameter ($H = 0.01$) the average Nusselt number of the solid phase is almost constant and not dependent on how much the Péclet number is for both aiding and opposing flows. This is because the solid phase temperature field is approximately not affected by the fluid phase temperature field due to small values of the heat transfer coefficient between the two phases as shown in Figs. 3(a) and 4(a) for aiding and opposing flows respectively. On the other hand the values of the average Nusselt number of the fluid phase is approximately equal to those of the equilibrium model results obtained by Lai et al. [7] for $Ra = 50$, $K_r = 1$ and $H = 0.01$. In the equilibrium model the solid temperature and the fluid temperature is assumed to be equal and hence the last term in the right hand side of Eq. (8) is zero in this case. The last term in the right hand side of Eq. (8) approaches zero also when H approaches zero and the results approach the equilibrium model results as shown in Fig. 2. The total average Nusselt number is exactly in between the corresponding values of solid and fluid phases according to Eq. (14) as shown in Fig. 2 for both aiding and opposing flows. Therefore, the thermally non-equilibrium effects are very strong for small values of heat transfer coefficient parameter H as shown in Figs. 2, 3(a) and 4(a). As the heat transfer coefficient parameter increases the average Nusselt number of the solid phase increases and the average Nusselt number of the fluid phase decreases, as shown in Fig. 2. At high values of H the values of the average Nusselt number of the both phases approaches each other and at very large values of H

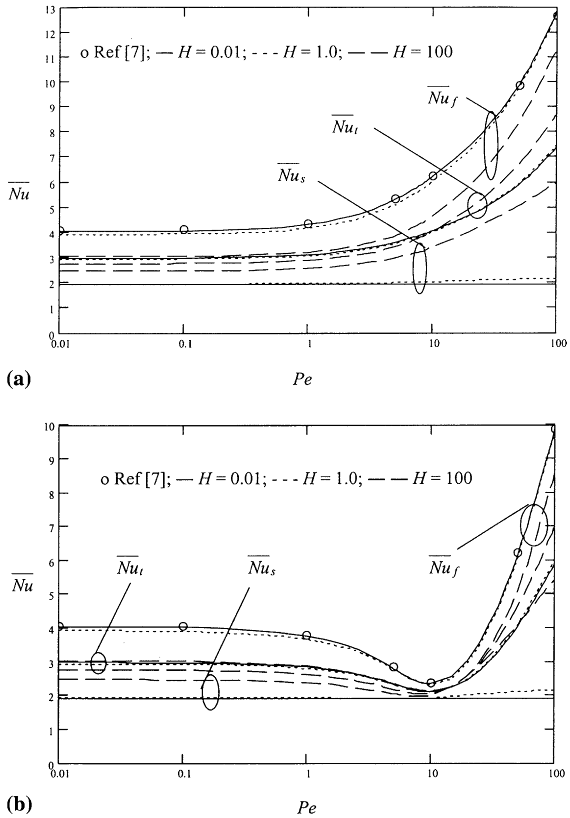

Fig. 2. Effect of H on the variation of average Nusselt number with Péclet number with $Ra = 50$ and $K_r = 1.0$: (a) aiding flow, (b) opposing flow.

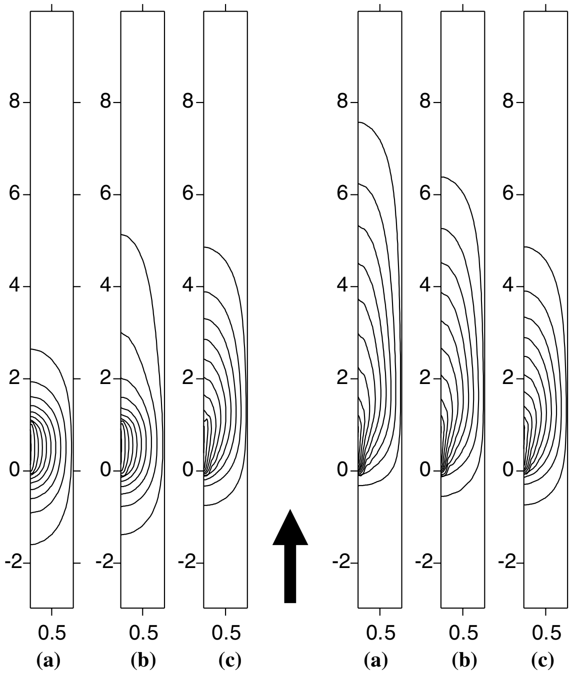

Fig. 3. Temperature field (θ_s left, θ_f right) for $Ra = 50$, $Pe = 1$, $K_r = 1.0$. Aiding flow ($\Delta\theta_f = \Delta\theta_s = 0.1$): (a) $H = 0.01$, (b) $H = 1$, (c) $H = 100$.

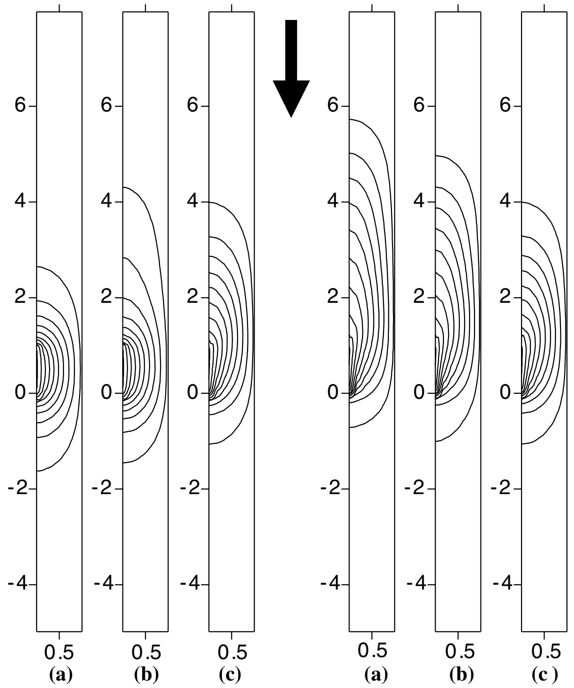

Fig. 4. Temperature field (θ_s left, θ_f right) for $Ra = 50$, $Pe = 1$, $K_r = 1.0$. Opposing flow ($\Delta\theta_f = \Delta\theta_s = 0.1$): (a) $H = 0.01$, (b) $H = 1$, (c) $H = 100$.

(or more specifically very high values of $H \times K_r$) the thermally equilibrium model can predict correctly the temperature fields and the average Nusselt number. Figs. 3(c) and 4(c) show the temperature fields of both the solid and the fluid fields at $H = 100$ for aiding and opposing flows respectively at $Ra = 50$, $Pe = 1$ and $K_r = 1$. It can be seen that these temperature fields are almost similar for both phases in the two cases of aiding and opposing flows, which reflect the thermally equilibrium case.

It is observed from Fig. 2 that the variation of the average Nusselt number for the fluid phase with the heat transfer coefficient parameter is less for high values of Pe than those at low values of Pe. For the solid phase the trend is opposite and the variation of $\overline{Nu}_s$ with H is more for high values of Pe than those at low values of Pe. As a result of these variations, the total average Nusselt number is affected by the heat transfer coefficient parameter for the forced convection mode (high Pe) more than the free convection mode (low Pe). Fig. 2 shows also that for both the aiding and opposing flows, the total average Nusselt number is decreasing with increasing the heat transfer coefficient parameter at low values of Pe, while for Pe more than 10, higher H will enhance the total heat transfer rate. It is important to note that, in practice, increasing the Péclet number leads to increasing the heat transfer coefficient between the two phases. The parameter H is expected to be higher in the forced convection than free convection.

4.2. Effect of thermal conductivity ratio parameter K_r

Figs. 5 and 6 show the effect of thermal conductivity ratio on the variation of the total average Nusselt number with Péclet number and with constant heat transfer coefficient parameter $H = 1$ for aiding and opposing flows respectively. For both aiding and opposing flows

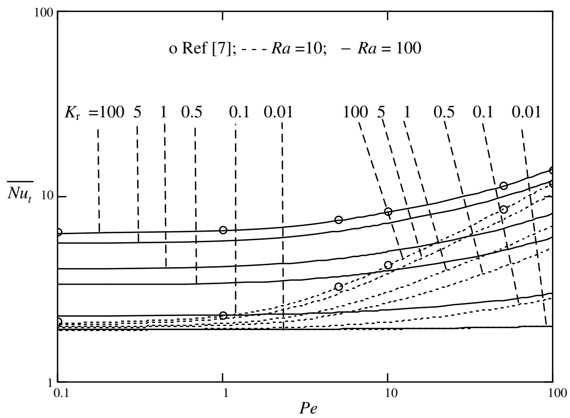

Fig. 5. Effect of K_r on the variation of total average Nusselt number with Péclet number with $H = 1$ aiding flow.

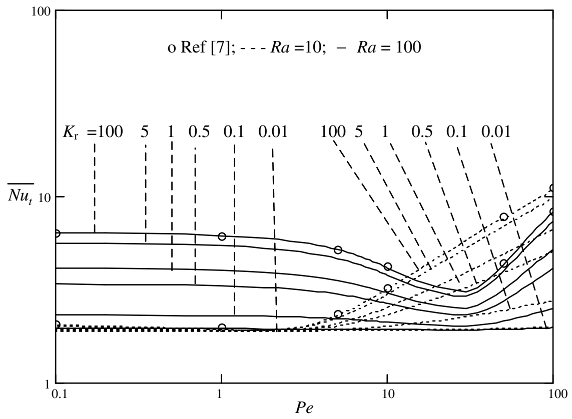

Fig. 6. Effect of K_r on the variation of total average Nusselt number with Péclet number with $H = 1$ opposing flow.

the values of the total Nusselt number for small values of K_r will be small compared with higher values of K_r as shown in Figs. 5 and 6 respectively. Increasing the thermal conductivity ratio leads to increase in the total average Nusselt number and at $K_r = 100$ the equilibrium model results are reproduced. This is due to the fact that the porous medium, with low porosity φ and/or low thermal conductivity of the fluid compared to that of solid, has low thermal conductivity ratio parameter K_r for example the metal foams. In this case the thermal resistance of the solid phase is the minimum and most of the heat will be carried out by conduction through the solid phase and partly by the fluid phase. In this case also, the average Nusselt number of the solid phase is almost constant and not dependent on how much the Péclet number is for both aiding and opposing flows. The solid phase temperature field is approximately not affected by the fluid phase temperature field due to low porosity φ and/or highly conductive solid phase as shown in Figs. 7(a) and 8(a) for aiding and opposing flows respectively.

On the other hand, porous medium with high porosity φ and/or high thermal conductivity of the fluid compared to that of solid has high K_r for example the grain storage. In this case the thermal resistance of the fluid phase is the minimum and most of the heat will be carried out by the fluid convection and partly by conduction through the solid phase. Figs. 5 and 6 show the variation of the total average Nusselt number with Péclet number with $K_r = 100$ is representing the results of the thermally equilibrium model by Lai et al. [7] for aiding and opposing flows respectively. The heat transfer between the two phases with high values of K_r (or more specifically with high values of $H \times K_r$) leads to the temperature fields of the two phases to be similar. Figs. 7(c) and 8(c) show that for $Ra = 10$, $Pe = 10$, $H = 1$ and $K_r = 100$, the solid and fluid temperature fields are

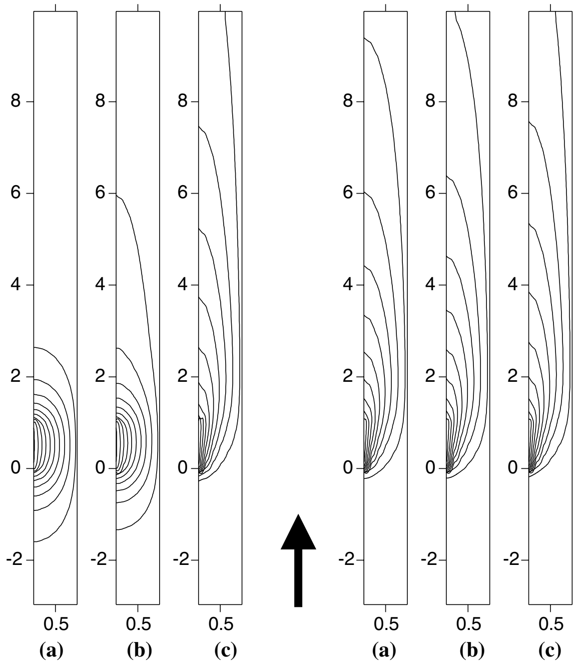

Fig. 7. Temperature field (θ_s left, θ_f right) for $Ra = 10$, $Pe = 10$, $H = 1.0$. Aiding flow ($\Delta\theta_f = \Delta\theta_s = 0.1$): (a) $K_r = 0.01$, (b) $K_r = 1$, (c) $K_r = 100$.

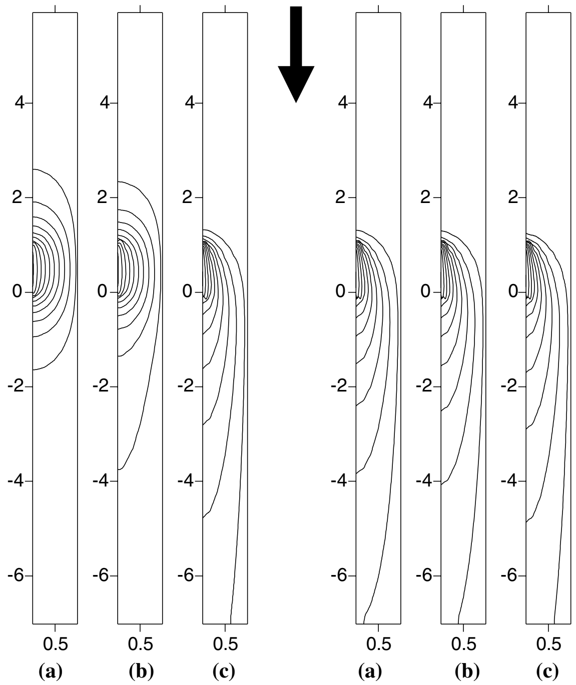

Fig. 8. Temperature field (θ_s left, θ_f right) for $Ra = 10$, $Pe = 10$, $H = 1.0$. Opposing flow ($\Delta\theta_f = \Delta\theta_s = 0.1$): (a) $K_r = 0.01$, (b) $K_r = 1$, (c) $K_r = 100$.

almost similar which indicates thermal equilibrium condition for both aiding and opposing flows. It can be seen that the thermally non-equilibrium condition is strong for small values of K_r (or more specifically with small values of $H \times K_r$) for both aiding and opposing flows.

Figs. 5 and 6 also show the effect of the Rayleigh number on the total average Nusselt number for aiding and opposing flows respectively. In the case of aiding flow, Fig. 5 shows that, for fixed values of H and K_r the difference in the total average Nusselt number is largest for small values of Péclet number (free convection), and this difference diminishes with an increase in Péclet number (forced convection). In the case of the opposing flow, Fig. 6 shows that, for fixed values of H and K_r the total average Nusselt number for a lower Rayleigh number ($Ra = 10$) is more than that for higher Rayleigh number ($Ra = 100$) in the mixed convection regime ($Pe > 20$). This observation has been noted by Lai et al. [7] in the thermal equilibrium model analysis. Another observation is made, when Rayleigh number is small ($Ra = 10$) the effect of K_r is not that significant for small Pe as that when Pe is large as shown in Figs. 5 and 6 for aiding and opposing flows respectively. For $Ra = 100$ the effect of K_r is clear and as mentioned earlier higher values of K_r enhanced the heat transfer even when $Pe = 0.01$ as shown in Figs. 5 and 6 for aiding and opposing flows respectively.

Finally the following comparison of the effect of the two parameters in the non-equilibrium model has been made. The increase of K_r from 0.01 to 100 leads to an increase of the total average Nusselt number by a factor of 2 or more for moderate Péclet number for example $Pe = 10$ as shown in Figs. 5 and 6 for aiding and opposing flows respectively. While the same increase in H is approximately not effected the values of the total average Nusselt number as shown in Fig. 2. These results reveal that the total average Nusselt number depends strongly on the thermal conductivity ratio parameter and depends slightly on the heat transfer coefficient parameter.

5. Conclusions

Numerical investigation have been carried out for two-dimensional steady mixed convection in a vertical porous layer using the thermally non-equilibrium model. The vertical porous layer is assumed to have a finite isothermally heated segment on one vertical wall which is otherwise adiabatic and the other vertical wall is cooled isothermally. The results show that, the thermal equilibrium model cannot predict the average Nusselt number correctly for small values of $H \times K_r$ in both the aiding and opposing flows. At high values of $H \times K_r$ the thermally equilibrium model can predict correctly the temperature fields and the average Nusselt number. For fixed values of H and K_r the difference in the total average Nusselt number is largest for small values of Péclet number (free convection), and this difference diminishes with an increase in Péclet number (forced convection). In the case of the opposing flow, for fixed values of H and K_r, the total average Nusselt number for a lower Rayleigh number ($Ra = 10$) is more than that for higher Rayleigh number ($Ra = 100$) in the mixed convection regime ($Pe > 20$). When Rayleigh number is small ($Ra = 10$), the effect of K_r is not significant in the free convection (small Pe) as that in the forced convection (large Pe) for aiding and opposing flows. For $Ra = 100$ the effect of K_r is clear and higher values of K_r enhanced the heat transfer even when $Pe = 0.01$ for aiding and opposing flows. It is observed also that, the total average Nusselt number depends strongly on the thermal conductivity ratio parameter and depends slightly on the heat transfer coefficient parameter.

References

[1] D.A. Nield, A. Bejan, Convection in Porous Media, second ed., Springer, Berlin, 1999.

[2] K. Vafai (Ed.), Handbook of Porous Media, Marcel Dekker, New York, 2000.

[3] I. Pop, D.B. Ingham, Convective Heat Transfer: Mathematical and Computational Modelling of Viscous Fluids and Porous Media, Pergamon, Oxford, 2001.

[4] D.B. Ingham, I. Pop (Eds.), Transport Phenomena in Porous Media, vol. 2, Pergamon, Oxford, 1998, p. 2002.

[5] A. Bejan, A.D. Kraus (Eds.), Heat Transfer Handbook, Wiley, New York, 2003.

[6] F.C. Lai, F.A. Kulacki, V. Prasad, Mixed convection in saturated porous media, in: S. Kakaç, B. Kilkis, F.A. Kulacki, F. Arinç (Eds.), Convective Heat and Mass Transfer in Porous Media, Kluwer, Dordrecht, 1991, pp. 225–287.

[7] F.C. Lai, V. Prasad, F.A. Kulacki, Aiding and opposing mixed convection in a vertical porous layer with a finite wall heat source, Int. J. Heat Mass Transfer 31 (1988) 1049–1061.

[8] F.C. Lai, C.Y. Choi, F.A. Kulacki, Free and mixed convection in horizontal porous layers with multiple heat sources, J. Thermophys. 4 (1990) 221–227.

[9] F.C. Lai, F.A. Kulacki, Oscillatory mixed convection in horizontal porous layers heated from below, Int. J. Heat Mass Transfer 34 (1991) 887–890.

[10] F.C. Lai, Mixed convection in saturated porous media, in: K. Vafai (Ed.), Handbook of Porous Media, Marcel Dekker, New York, 2000, pp. 605–661.

[11] V. Prasad, F.-C. Lai, F.A. Kulacki, Mixed convection in horizontal porous layers heated from below, ASME J. Heat Transfer 110 (1988) 395–402.

[12] A.A. Mohamad, S. Ramadhyani, R. Viskanta, Modelling of combustion and heat transfer in a packed bed with embedded coolant tubes, Int. J. Heat Mass Transfer 37 (1994) 1181–1197.

[13] K. Vafai, M. Sozen, Analysis of energy and momentum transport for fluid flow through a porous bed, ASME J. Heat Transfer 112 (1990) 690–699.
[14] M. Kaviany, Principles of Heat Transfer in Porous Media, second ed., Springer, New York, 1999.
[15] T.E.W. Schumann, Heat transfer: a liquid flowing through a porous prism, J. Franklin Inst. 208 (1929) 405–416.
[16] A. Amiri, K. Vafai, Analysis of dispersion effects and non-thermal equilibrium, non-Darcian, variable porosity incompressible flow through porous media, Int. J. Heat Mass Transfer 37 (1994) 939–954.
[17] A. Amiri, K. Vafai, Transient analysis of incompressible flow through a packed bed, Int. J. Heat Mass Transfer 41 (1998) 4259–4279.
[18] W.J. Minkowycz, A. Haji-Sheikh, K. Vafai, On departure from local thermal equilibrium in porous media due to a rapidly changing heat source: the Sparrow number, Int. J. Heat Mass Transfer 42 (1999) 3373–3385.
[19] A.A. Mohamad, Nonequilibrium natural convection in a differentially heated cavity filled with a saturated porous media, ASME J. Heat Transfer 122 (2000) 380–384.
[20] P.X. Jiang, Z.P. Ren, Numerical investigation of forced convection heat transfer in porous media using a thermal non-equilibrium model, Int. J. Heat Fluid Flow 22 (2001) 102–110.
[21] S.J. Kim, S.P. Jang, Effect of the Darcy number, the Prandtl number, and the Reynolds number on local thermal non-equilibrium, Int. J. Heat Mass Transfer 45 (2002) 3885–3896.
[22] B. Alazmi, K. Vafai, Constant wall heat flux boundary conditions in porous media under local thermal non-equilibrium conditions, Int. J. Heat Mass Transfer 45 (2002) 3071–3087.
[23] N. Banu, D.A.S. Rees, Onset of Darcy–Benard convection using a thermal non-equilibrium model, Int. J. Heat Mass Transfer 45 (2002) 2221–2228.
[24] A.C. Baytas, I. Pop, Free convection in a square porous cavity using a thermal nonequilibrium model, Int. J. Therm. Sci. 41 (2002) 861–870.
[25] A.A. Mohamad, Natural convection from a vertical plate in a saturated porous medium, Non-equilibrium theory, J. Porous Media 4 (2001) 181–186.
[26] L.B. Younis, R. Viskanta, Experimental determination of the volumetric heat transfer coefficient between stream of air and ceramic foam, Int. J. Heat Mass Transfer 36 (1993) 1425–1434.
[27] B.M. Galitseisky, A.L. Loshkin, Unsteady method of experimental investigation of heat transfer in porous material, in: J. Padet, F. Arinc (Eds.), Int. Symp. on Transient Convective Heat Transfer, 1997, pp. 201–214.
[28] C.C. Wu, G.J. Hwang, Flow and heat transfer characteristics inside packed and fluidized beds, ASME J. Heat Transfer 120 (1998) 667–673.
[29] S.V. Patankar, Numerical Heat Transfer and Fluid Flow, McGraw-Hill, New York, 1980.
[30] T. Hayase, J.A.C. Humphrey, R. Greif, A consistently formulated QUICK scheme for fast and stable convergence using finite-volume iterative calculation procedures, J. Comput. Phys. 98 (1992) 108–118.